

LETTER TO THE EDITOR

The first brown dwarf with a disk in Chamaeleon II^{★,★★}

J. M. Alcalá¹, L. Spezzi², A. Frasca³, E. Covino¹, A. Porras⁴, B. Merín⁵, and P. Persi⁶

¹ INAF - Osservatorio Astronomico di Capodimonte, via Moiariello 16, 80131 Napoli, Italy
e-mail: jmae@na.astro.it

² Dipartimento di Fisica e Astronomia, Università di Catania, via S. Sofia, 78, 95123 Catania, Italy

³ INAF - Osservatorio Astrofisico di Catania, via S. Sofia, 78, 95123 Catania, Italy

⁴ Center for Astrophysics, Harvard

⁵ Leiden Observatory, PO Box 9513, 2300 RA Leiden, The Netherlands

⁶ INAF – IASF Roma, via fosso del cavaliere, 100, 00133 Roma, Italy

Received 27 March 2006 / Accepted 20 April 2006

ABSTRACT

In this letter we characterize the candidates for young stars and brown dwarfs detected in a survey with ISOCAM in the Chamaeleon II dark cloud. Photometric data coming from a wide-field optical imaging survey, combined with IR measurements from the 2MASS catalogue and from the *Spitzer* satellite, allow us to study the nature of the candidates. Using intermediate-band filters we can provide a first estimate of the temperatures for objects cooler than about 3800 K. On the basis of spectroscopic and photometric data, we confirm that ISO-CHA II 13 is a young substellar object with a mass of about $0.05 M_{\odot}$. It is thus the first object in Cha II whose substellar nature has been spectroscopically confirmed. By having a temperature of about 2880 K and displaying a substantial infrared excess, it joins the list of young brown dwarfs observed to have a surrounding disk.

Key words. stars: low-mass, brown dwarfs – stars: formation – stars: pre-main sequence – stars: individual objects: ISO-CHA II 13

1. Introduction

The search for young brown dwarfs (BDs) has recently become an important issue in addressing the problem of disk frequency in young substellar objects. It takes advantage of the fact that young BDs in star-forming regions (SFRs) at ages of a few Myr have luminosities between 10^4 and 10^5 times higher than when they are old (Burrows 2001).

Because of its proximity to the Sun ($d = 178$ pc; Whittet et al. 1997), the Cha II dark cloud is particularly well-suited for seeking young BDs and for doing research on disk frequency in the sub-stellar regime. The region is characterized by the presence of H α -emission stars (Hartigan 1993), of embedded class-I and class-II infrared (IR) sources (Larson et al. 1998), as well as of X-ray-emitting young stellar objects (Alcalá et al. 2000).

Previous investigations in the near IR by the DENIS survey have revealed several candidates for classification as young BDs in Cha II (Vuong et al. 2001). However, a spectroscopic follow-up of several of these candidates failed to find young BDs (Barrado y Navascués & Jayawardhana 2004). These follow-up observations revealed, however, the least massive classical T Tauri star in the cloud. Persi et al. (2003) performed ISOCAM observations and IR spectroscopy of objects in the core of Cha II and found a number of sources with IR excess, among which is ISO-CHA II 13, a promising candidate for a BD. Cha II has also been surveyed during the *c2d Spitzer* legacy survey (Evans et al. 2003; Young et al. 2005; Allers et al. 2006).

In this letter we report the first spectroscopically confirmed BD with a disk in Cha II.

2. Optical imaging

The imaging data used in this letter are part of an optical imaging survey in Cha II performed with the Wide-Field Imager (WFI) at the ESO 2.2 m telescope in the R_c , I_c , z broad bands, in the H α (broad and narrow) and 856-nm and 914-nm intermediate-band filters. The sky area surveyed with WFI in Cha II is about 2 square degrees and covers the cloud almost entirely. The details of the optical survey will be presented in a forthcoming paper. Table 1 reports the objects investigated in the present work.

Except for ISO-CHA II 13, which is barely seen in the R -band but not detected in the H α images, the other three objects are clearly seen in all the WFI images. ISO-CHA II 98 appears as a visual binary (separation $\leq 0.8''$). Thus, its photometric measurements must be taken with care.

The ($m_{856} - m_{914}$) index is very sensitive to the effective temperature for very cool stars ($T_{\text{eff}} < 3800$ K) since the 856-nm filter includes a strong TiO molecular band whose intensity grows with decreasing temperature (O'Neal et al. 1998). The diagram in Fig. 1 shows the relation between the ($m_{856} - m_{914}$) index and the effective temperature (shaded area), determined by us using the filter transmission curves for the corresponding WFI intermediate-band filters and the synthetic low-resolution StarDusty spectra for low-mass stars and BDs (Allard et al. 2000). This relation is slightly dependent on the stellar gravity. We also derived the relationship using other stellar atmosphere models (e.g. NextGen, COND, etc.), while the StarDusty models were selected because they match the empirical relationship better between the ($m_{856} - m_{914}$) index and effective temperature

* Based on observations carried out at the European Southern Observatory under programs 67.C-0225, 68.C-0311, and 276.C-5021.

** Table 2 and Fig. 4 are only available in electronic form at <http://www.edpsciences.org>

Table 1. Photometry of the studied objects. Decimal errors are given in parentheses.

| ISO-CHA II | RA(2000) | Dec(2000) | R_c | I_c | z | m_{856} | m_{914} |
|------------------|------------|-----------|------------|------------|------------|------------|------------|
| 13 | 12:58:06.8 | -77:09:09 | 22.51(.27) | 19.38(.06) | 17.89(.04) | 19.44(.19) | 18.33(.11) |
| 73 | 13:01:46.2 | -77:16:03 | 16.31(.02) | 15.12(.01) | 14.68(.01) | 15.38(.09) | 15.13(.08) |
| 98 | 13:03:26.0 | -77:01:48 | 15.22(.01) | 14.98(.01) | 12.97(.02) | 15.76(.10) | 15.36(.09) |
| 110 [†] | 13:04:19.2 | -77:54:00 | 14.52(.01) | 14.03(.01) | 14.03(.01) | — | — |

[†] Not observed in intermediate bands. Temperature derived by fitting the StarDusty spectrum to the observed SED.

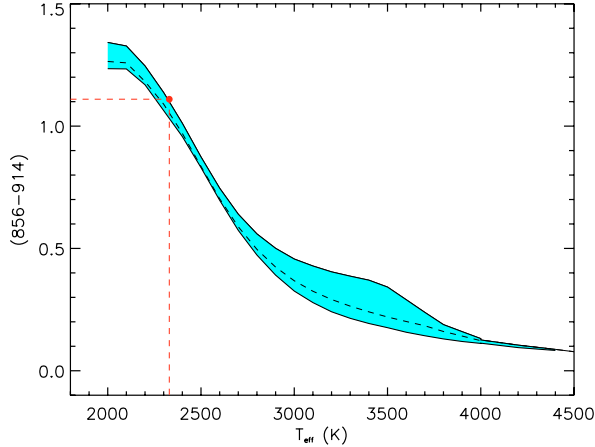


Fig. 1. $m_{856} - m_{914}$ index versus effective temperature relation derived from the corresponding WFI intermediate-band filters and the synthetic low-resolution StarDusty spectra for low-mass stars and BDs by Allard et al. (2000). The two solid lines show the relation for $\log g = 5.0$ (lower boundary) and $\log g = 3.5$ (upper boundary); the dashed line represents the T_{eff} -color relation for $\log g = 4.0$. The point represents the observed color index for ISO-CHA II 13.

by López-Martí et al. (2004). Furthermore, Allard et al. (2001) found that silicate dust grains can form abundantly in the outer atmospheric layers of the latest M dwarfs and BDs.

We can thus estimate a temperature for our targets by assuming $\log g = 3.5$ ¹ and thereby preselecting very cool candidates. However, in the case of high extinction the temperature derived in this way may be underestimated, because the $m_{856} - m_{914}$ index becomes larger than in the absence of extinction. Thus, we only use these temperature estimates to preselect potential BD candidates. The most interesting object among those reported here is indeed ISO-CHA II 13, for which a temperature of 2330 ± 200 K is derived. All the other objects turn out to have a temperature higher than 3200 K.

3. Spectroscopy

In order to investigate the nature of ISO-CHA II 13 in more detail, we performed spectroscopic observations using FORS2 at the ESO-VLT under director's discretionary time (DDT). The observations consisted of two observing blocks (OBs) of 40 min each. The resolution measured from the HeAr lines is about 9 Å (FWHM) in the spectral range 6100–10000 Å. One OB was performed on the night of 23 January 2006 and the other on 2 February 2006. The stars Feige 66 and LTT 4816 were observed with the same instrumental set-up for relative flux calibration during the first and second OB, respectively. The data reduction was performed with MIDAS and IRAF. From the

¹ According to Baraffe et al. (2003), this value of gravity is appropriate for very young sub-stellar objects.

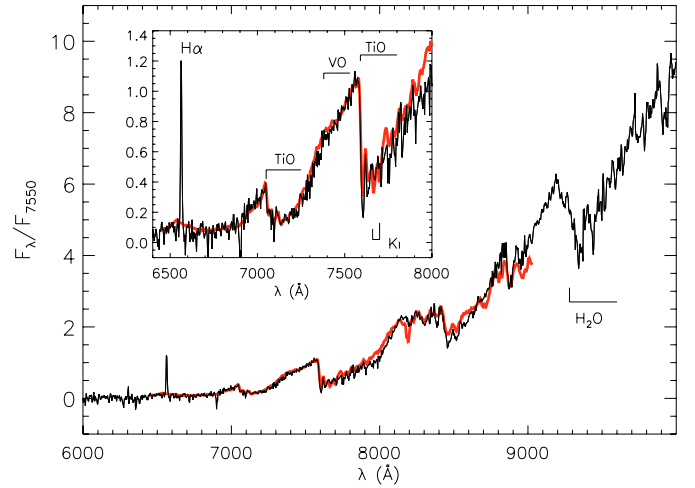


Fig. 2. Optical spectrum of ISO-CHA II 13 (thin line). Note the strong H α emission. Overplotted with a thick line is the best-fitted average M7 template, reddened at $A_V = 5.0$. The spectra are normalized to the flux at 7550 Å.

optical spectrum, shown in Fig. 2, one can immediately recognize a very late-type spectrum and signatures of a high level of activity: we observe strong H α emission ($EW = 100 \pm 20$ Å) and some indication of the Ca II IR triplet in emission (e.g. Fig. 4²).

We derived the spectral type of ISO-CHA II 13 by means of a fitting procedure developed by us in the IDL environment, which provides us with the best spectral type and interstellar extinction by χ^2 minimization. In this procedure, which is a variation of the ROTFIT code described by Frasca et al. (2003), we used as reference a grid of templates constructed by averaging spectra of dwarf and giant stars, following the prescription by Luhman et al. (1999, 2003) and Guieu et al. (2006). The grid of templates was fixed by collecting spectra of dwarfs and giants from Kirkpatrick et al. (1999), Martin et al. (1999), Legget et al. (2000), and Fluks et al. (1994). For the reddening, we used the extinction law by Cardelli et al. (1989). The best-fit spectrum corresponds to an average M7 template with a visual extinction $A_V = 5.0 \pm 0.5$ mag. We verified this independently for the two spectra obtained. The Na I and K I absorption lines at around $\lambda = 8230$ Å and $\lambda = 7699$ Å, respectively, are intermediate in strength between those of dwarfs and giants, as expected for a young object. From the spectral type versus temperature relation by Luhman et al. (2003), we derived a temperature for ISO-CHA II 13 of 2880 ± 70 K, which is higher than the one obtained from the $(m_{856} - m_{914})$, mainly for two reasons: *i*) the extinction and *ii*) the differences between the temperature derived from model atmospheres and from template spectra.

Based on a fit to the spectral energy distribution, Allers et al. (2006) derived $A_V = 10$ mag and a temperature of 2925 K for

² Published only in electronic form.

ISO-CHA II 13. Although their temperature estimate is roughly consistent with our results, the extinction estimate derived by Allers et al. is a factor of two higher. An average template spectrum corresponding to a temperature of 2925 K with $A_V = 10$ does not fit the optical spectrum. Using the temperature of 2880 K for ISO-CHA II 13, and the intrinsic color versus spectral type relation by Luhman et al. (2003), we independently estimate a visual extinction $A_V = 4.6 \pm 0.5$ mag, which is consistent within the errors with the above result of our two-parameter fit. Note that, besides the higher temperature, Allers et al. report an *I*-band magnitude that is 0.23 mag fainter than ours. Such differences in photometry and temperature may lead to a difference in extinction of up to 1 mag.

Although extinction maps measure only the global extinction in the general location of a given object, so are not very sensitive to local variations, we note that our A_V estimate is consistent with the map reported by Cambrésy (1999). Thus, in the following analysis, we adopt the temperature and extinction derived from the spectroscopic data above.

4. Physical parameters

In order to derive the spectral energy distribution (SED) of ISO-CHA II 13, we first corrected the observed flux at each wavelength for interstellar extinction, adopting $A_V = 5.0$. From our analysis we find that ISO-CHA II 13 shows an IR excess, indicating the presence of a disk. The SED of ISO-CHA II 13 is shown in Fig. 3; the data from the 2MASS catalogue, ISOCAM, and the *Spitzer* satellite are included³. For details on the extraction of the *Spitzer* data see Porras et al. (2006, in preparation). The *Spitzer* colors $[3.6] - [4.5] = 0.45$ and $[3.6] - [4.5] = 0.60$ of ISO-CHA II 13 are consistent with those of other BDs with disks (cf. Hartmann et al. 2005).

The luminosity of ISO-CHA II 13 was first estimated by fitting a StarDusty model of the same temperature to the SED. The fit was performed on the short-wavelength portion ($\lambda \leq \lambda_j$) of the SED, which is less contaminated by an eventual IR excess. The corresponding best-fit is also shown in Fig. 3. Integrating the StarDusty spectrum and assuming the distance of 178 ± 18 pc for the Cha II cloud (Whittet et al. 1997), we derive a luminosity of $0.009 \pm 0.002 L_\odot$. In addition to this estimate, we also evaluated the “total” luminosity of $0.024 \pm 0.005 L_\odot$ by direct integration of the observed SED. The difference between the luminosity of the StarDusty model and the one obtained from integration of the SED may be attributed to the luminosity of the disk.

The strong $H\alpha$ emission and IR excess of ISO-CHA II 13, as well as its intermediate gravity between dwarfs and giants witnessed by the weak NaI and KI absorption lines, provide strong support for a young age and thus for membership in the Cha II cloud. By comparing the location on the HR diagram with the evolutionary tracks by Baraffe et al. (2003), we derived an age of 5 ± 3 Myr and a mass $M \approx 0.05 M_\odot \pm 0.01$, from which we conclude that ISO-CHA II 13 is indeed the first spectroscopically confirmed substellar object, showing signatures of accretion, in the Cha II region.

5. Discussion

Based on its low mass ($0.05 \pm 0.01 M_\odot$) and the presence of mid-IR excess emission, ISO-CHA II 13 is the first clear example of

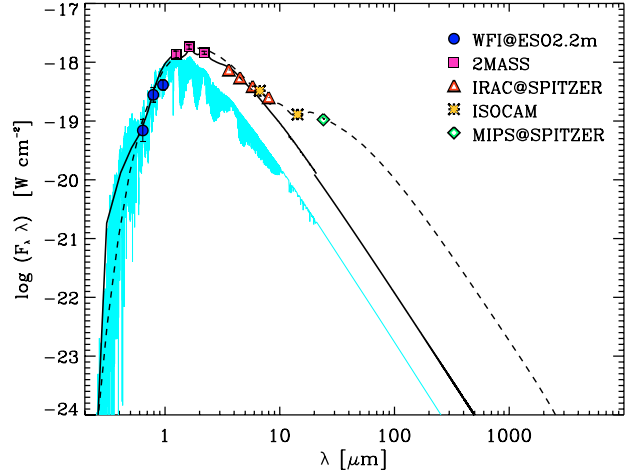


Fig. 3. Spectral energy distribution of ISO-CHA II 13. The StarDusty spectrum with the same temperature as the BD is over-plotted. The continuous line is the sum of the star and disk emissions assuming black-body emission from the disk, while the dashed line is the result of the fit performed with the FitCGplus tool by Dullemond et al. (2001).

a young brown dwarf with a circumstellar disk in the Cha II star-forming region.

As a starting point for further investigating the disk around ISO-CHA II 13, we determined the excess luminosity due to the disk as $L_{\text{disk}}(\lambda) = 4\pi d^2 \Delta f(\lambda)$, where $\Delta f(\lambda)$ is the excess between the dereddened observed flux and the flux of the StarDusty model at each wavelength. We then fitted the $L_{\text{disk}}(\lambda)$ distribution by assuming black-body emission, where the free parameters are the temperature, T_{disk} , and the projected emitting area $A_{\text{projected}} = A_{\text{disk}} \cdot \cos i$, with i the inclination angle. Assuming that the disk is thin, the effective area emitting in the whole solid angle would be $A_{\text{disk}} = 2\pi(R_{\text{out}}^2 - R_{\text{in}}^2)$, where R_{out} and R_{in} are the inner and outer radii of the disk. Assuming that $R_{\text{in}} = R_\star = 0.38 R_\odot$, we made calculations using two inclination angles, namely $i = 0$ and $i = 1 \text{ rad} = 57.3^\circ$, the latter being the average value for randomly distributed inclinations. In the case of $i = 0$, our best-fit yields $R_{\text{out}} = 2.0 R_\odot$, while we obtain $R_{\text{out}} = 2.6 R_\odot$ for $i = 57.3^\circ$. The disk temperature we derived in this way is on the order of $T_{\text{disk}} \approx 1600$ K, still consistent with the disk models for BDs (see Fig. 1 by Walker et al. 2004). Our best fit (star+disk) is shown in Fig. 3.

The simple assumption of isothermal black-body radiation neglects any radial temperature distribution, but it is a good starting point for understanding the physical properties of ISO-CHA II 13 and its disk. Thus, since the IR excess is dominated by the hot component of the disk, the disk-size we obtain should correspond to the inner wall, while the temperature should be closer to the maximum temperature of a possibly flared disk. We have then used the above values for the disk and stellar parameters as the starting point of a SED fit using the FitCGplus model tool for proto-planetary disks by Dullemond et al. (2001). The best-fit corresponds to a flared disk with an inner disk temperature of 1500 K, radius of $85 R_\odot$ (≈ 0.4 AU), mass of $0.0001 M_\odot$, and inclination of 58° (although we find that the inclination angle has little impact on the SED). The SED derived in this way is also found in Fig. 3. More sophisticated disk models will provide more detailed information on the disk parameters related to mass accretion.

Acknowledgements. This work was partially financed by INAF and COFIN-MIUR. We thank the referee, K. Luhman, for his useful comments and suggestions. Support for this work, part of the Spitzer Legacy Science Program,

³ The data are reported in Table 2, which is only provided in electronic form.

was provided by NASA through contract 1224608 issued by the Jet Propulsion Laboratory, California Institute of Technology, under NASA contract 1407. We thank Neal Evans, PI of the c2d Legacy Program, and the Lorentz Center in Leiden for hosting several meetings that contributed to this paper. B.M. acknowledges the Fundación Ramón Areces for a post-doctoral grant. We thank M. Arnaboldi for help with the ESO OBS. This research made use of the NASA/IPAC Infrared Science Archive, which is operated by the Jet Propulsion Laboratory, California Institute of Technology, under contract with NASA.

References

- Alcalá, J. M., Covino, E., Sterzik, M. F., et al. 2000, *A&A*, 355, 629
Allard, F., Hauschildt, P. H., & Schwenke, D. 2000, *ApJ*, 540, 1005
Allard, F., Hauschildt, P. H., Alexander, D. R., et al. 2001, *AJ*, 556, 357
Allers, K. N., Kessler-Silacci, J. E., Cieza, L. A., & Jaffe, D. T. 2006, *ApJ*, in press
Baraffe, I., Chabrier, G., Barman, T. S., Allard, F., & Hauschildt, P. H. 2003, *A&A*, 402, 701
Barrado y Navascués, D., & Jayawardhana, R. 2004, *ApJ*, 615, 840
Burrows, A. 2001, *Rev. Mod. Phys.*, 73(3), 719
Cambrésy, L. 1999, *A&A*, 345, 965
Cardelli, J. A., Clayton, G. C., & Mathis, J. S. 1989, *ApJ*, 345, 245
Dullemond, C. P., Dominik, C., & Natta, A. 2001, *ApJ*, 560, 969
Evans II, N. J., Allen, L., Blake, G. A., et al. 2003, *PASP*, 115, 965
Fluks, M. A., Plez, B., The, P. S., et al. 1994, *A&AS*, 105, 311
Frasca, A., Alcalá, J. M., Covino, E., et al. 2003, *A&A*, 405, 149
Guieu, S., Dougados, C., Monin, J.-L., et al. 2006, *A&A*, 446, 485
Hartigan, P. 1993, *AJ*, 105, 1511
Hartmann, L., Megeath, S. T., Allen, L., et al. 2005, *ApJ*, 629, 881
Kirkpatrick, J. D., et al. 1999, *ApJ*, 519, 802
Larson, K. A., Whittet, D. C. B., Prusti, T., & Chiar, J. E. 1998, *A&A*, 337, 465
Leggett, S. K., Allard, F., Dahn, C., et al. 2000, *ApJ*, 535, 965
López-Martí, B., Eislöffel, J., Scholz, A., & Mundt, R. 2004, *A&A*, 416, 555
Luhman, K. L. 1999, *ApJ*, 525, 466
Luhman, K. L., Stauffer, J. R., Muench, A. A., et al. 2003, 593, 1093
Martín, E. L., Delfosse, X., Basri, G., et al. 1999, *AJ*, 118, 2466
Persi, P., Marenzi, A. R., Gómez, M., & Olofsson, G. 2003, *A&A*, 399, 995
O'Neal, D., Neff, J. E., Saar, S. H., et al. 1998, *ApJ*, 507, 919
Vuong, M. H., Cambrésy, L., Epchtein, N., et al. 2001, *A&A*, 379, 208
Walker, C., Wood, K., Lada, C. J., et al. 2004, *MNRAS*, 351, 607
Whittet, D. C. B., Prusti, T., Franco, G. A. P., et al. 1997, *A&A*, 327, 1194
Young, K. E., Harvey, P. M., Brooke, T. Y., et al. 2005, *ApJ*, 628, 283

Online Material

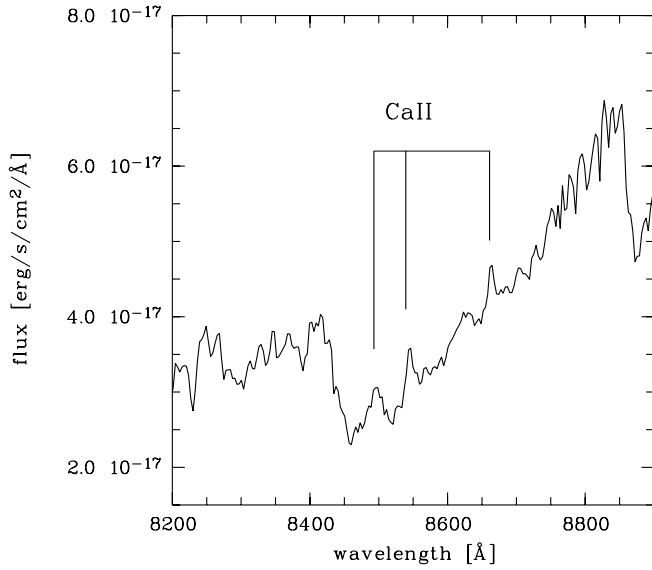


Fig. 4. Zoom of the spectrum in Fig. 2 showing the Ca II infrared triplet lines.

Table 2. Observed flux vs. wavelength of ISO-CHA II 13.

| Flux (mJy) | Wavelength (m μ) | ref. |
|---------------------|--------------------------|------|
| 0.0031 ± 0.0008 | 0.64 | a |
| 0.0441 ± 0.0024 | 0.79 | a |
| 0.1782 ± 0.0181 | 0.91 | a |
| 0.1810 ± 0.0067 | 0.96 | a |
| 1.5100 ± 0.0514 | 1.25 | b |
| 4.3200 ± 0.0836 | 1.62 | b |
| 6.0800 ± 0.1680 | 2.20 | b |
| 7.0000 ± 0.0687 | 3.60 | c |
| 6.9100 ± 0.0659 | 4.50 | c |
| 6.7100 ± 0.0586 | 5.80 | c |
| 6.7000 ± 0.6000 | 6.70 | d |
| 6.2500 ± 0.0417 | 8.00 | c |
| 6.0000 ± 1.2000 | 14.30 | d |
| 8.3900 ± 0.1400 | 24.00 | e |

References:

- a) this work;
- b) 2MASS catalog;
- c) IRAC@SPITZER, this work;
- d) ISOCAM data (Persi et al. 2003);
- e) MIPS@SPITZER (Young et al. 2005).